Extinction limits and structure of counterflow nonpremixed water-laden methane/air flames

R. E. Padilla[a], O. C. Kwon [b], S. Lee[c], D. Dunn-Rankin[a] , and T. K. Pham[d]

[a]*Department of Mechanical and Aerospace Engineering University of California, Irvine,CA 92697,USA*
[b]*School of Mechanical Engineering, Sungkyunkwan University, Suwon, Gyeonggi-do 440-746,Korea*
[c]*Department of Mechanical Engineering,Inha University, Incheon 402-751,Korea*
[d]*Department of Mechanical Engineering, California State University, Los Angeles, CA 90032,USA*

Abstract

In order to better understand nonpremixed combustion processes when large amounts (water/fuel molar ratios on the order of unity) of water naturally incorporate into the fuel stream, the extinction limits and structure of counterflow nonpremixed flames of mixtures of water vapor, methane and air were identified experimentally and computationally. Such conditions arise, for example, in the combustion of methane hydrates and water/fuel emulsions. With water vapor addition, the extinction limits and flame temperature and location of methane/air flames were experimentally determined, while the extinction limits and the detailed flame structure were computed using a detailed kinetic mechanism, including a statistical narrow-band radiation model. Results generally show narrowing of the extinction limits (in terms of the water to methane molar ratio) with increasing strain rates, implying that flames can sustain more water vapor at low strain rates. The maximum flame temperature at the extinction limit increases with increasing strain rate because there is less water present to act as a thermal sink. This result shows that the extinction is not due simply to water as a diluent but also involves reactant leakage. For a fixed strain rate, the maximum flame temperature decreases with water addition. With water addition flame location shifts towards the air stream due to the increased momentum of the water vapor-laden jet. Comparative predictions assuming added non-reactive water vapor indicate that the chemical effects of water addition on flame structure are relatively small but may be critical near extinction. Predicted and measured tendencies of extinction limits and temperature for various conditions exhibit encouraging agreement, but quantitative discrepancies among the predictions and measurements indicate a need in additional consideration for heat loss modeling.

1 Introduction

Interest in methane (CH_4) hydrate combustion has increased due to the extreme energy potential and environmental impact this fuel represents[1]. Burning methane hydrates involves a combustion process where a large amount of water (H_2O) is naturally incorporated into the fuel stream since, hydrates consist of 86% water and 14% methane by mole fractions [2]. While lower levels of water addition are involved than with hydrate flames, other examples of water-laden fuel nonpremixed flames include the combustion of water/fuel emulsions to mitigate nitrogen oxides (NOx) production and the rapidly rising fuel plume above LNG pool fires. Motivated by these combustion processes where water is incorporated on the fuel side of nonpremixed flames, this study will focus on examining the effects of water addition on the counterflow flame by adding water into the fuel stream. The desire to understand the interaction between water and flames has largely centered on fire suppression applications since water mists can be considered as a nontoxic, non-corrosive suppressant with zero ozone depletion and global warming risks, due to its significant cooling capacity and diluting effects of reactants in both liquid and vapor phases, reducing the adiabatic flame temperature [3−7]. These prior studies provide information such as limits of water mist concentration below which flames cannot be self-sustained, or droplet size and mist loading density for the best suppression performance to show that water mist is a potential candidate for replacing Halon 1301 suppressant [4−6].

Because past studies have focused on fire suppression and premixed engine applications, they have considered liquid water introduced into the air stream of counterflow flame burners, introduces water vapor into a heated fuel

Correspondence to:repadill@uci.edu

stream through the bottom nozzle of the counterflow flame burner.Specifically, we study experimentally water-laden nonpremixed methane/air flames under conditions close to those observed in methane hydrate combustion as this is the most extreme example of a natural fuel/water mixture nonpremixed flame. The extinction limits (in terms of the water to methane molar ratio) and flame temperature are measured, while computationally the extinction limits and the detailed flame structure is determined.

2 Experimental and computational methods

This experiment was performed using a counterflow burner (see Figure 1), which consists of a pair of main stainless steel tubes (nozzles), each surrounded with a concentric tube to provide sheath coflow of nitrogen (N_2). Honeycomb steel screens with a cell diameter of 0.062 in. were stretched tightly across on the exits of the fuel and oxidizer burners. In addition, two other screens are 2 in. apart within each burner to help make the internal flow uniform. Fuel with water vapor and air issue respectively from the bottom and top nozzles with the inner diameter $d = 19.$ mm and the nozzle separation distance L = 12.7 mm. The upper and lower inner tubes are aligned axially. The coflow injection velocity is adjusted to a point were a flat flame is obtained. The respective fuel and air injection velocities u_F and u_O reported are nominal values only and do not include the additional velocity produced when water vapor is added. Thus, the velocities and strain rates not constant. Future measurements will determine the velocity of fuel and water and air.

Commercial mass flow controllers deliver CH_4 (purity > 99.999%) and air (21% oxygen (O_2)/79% N_2 in volume, purity > 99.9%). Deionized liquid water is supplied into the fuel (CH_4) stream using a syringe pump and is vaporized using an electric furnace. Maximum flame temperature is measured with a B-type thermocouple. To confirm that water is prevaporized and that there is no indication of cold spots throughout the experimental apparatus, temperatures are monitored using type K thermocouples. The lower (fuel) nozzle is electrically heated and is thermally insulated, which keeps the burner heated as well as the reactants. For all experiments of water-laden CH_4/air nonpremixed flames, the strain rate identified is based on a fixed water-free u_F and u_O), although the H_2O to CH_4 molar ratio R_{H_2O/CH_4} is increased up to the point that the flame extinguishes. That is, the identified strain rate does not account for water addition. In the present study, the strain rate is defined as [9]:

$$a = \frac{-2u_o}{L}[1 - \frac{u_f}{u_o}(\frac{\rho_f}{\rho o})] \tag{1}$$

where ρ is the density and the subscripts F and O denote fuel and oxidizer (air), respectively. With this definition the effective fuel density changes slightly with water addition, but with the small molar mass difference between methane and water, this effect is very small. The larger effect would be the change in velocity associated with the water addition. The extinction limits (R_{H_2O/CH_4}, max) are measured for various strain rates, and for various a and H_2O/CH_4 conditions the temperature distribution, and thereby the maximum flame temperature (T_{max}), is measured. Final results are obtained by averaging measurements of 4 to 6 tests at each condition. Direct measurements showed that the fuel nozzle exit temperature is approximately T_F = 550.3 K and the air nozzle exit temperature T_O = 350.3 K. These temperatures are not constant,unfortunately,so reactants will become preheated and flame temperatures will vary with different fuel and water compositions. The temperatures are continuously monitored through out the experiment using a suite of type K thermocouples, which are positioned on the exits of the fuel and oxidizer burners. Thus, computations were carried out for these conditions. Atmospheric pressure (NP) was maintained throughout for a = $62-108$ s^{-1} (u =0.14$-$0.44 m/s) and R_{H_2O/CH_4} = 0$-$2.3. As described earlier, the reported strain rate is nominal and represents the initial strain rate before water is added into the fuel stream.

Computational methods are similar to past work [9, 10]; that is GRI Mech$-$3.0 and updated reaction coefficients have been implemented. Assuming that the radial velocity varies linearly in the radial direction, the two-dimensional flow analysis can be simplified and the fluid properties become functions of only the axial direction x. These resulting equations are then the same as those in [9]. Heat losses due to gas radiation are included in the energy equation and radiative transport, including both emission and absorption, is computed using the statistical narrow-band model with an exponential-tailed inverse line strength distribution [11]. The radiative transfer equations are solved using the method discussed by Soufiani et. al [12]. Convective and conductive heat losses were not considered because such losses would represent non-ideal experimental behavior. If the counterflow

flame is functioning properly, radiation should be the dominant heat transfer mechanism. The simulations were conducted using a revised code from the OPPDIF program [13]. The CHEMKIN package [14−16] is used as a preprocessor to find the thermochemical and transport properties for the code. All the calculations are carried out with a $CH_4/O_2/N_2$ mechanism involving 53 species and 325 reversible reactions [17].

3 Results and discussion

3.1 Flame morphology

Figure 2 shows counterflow nonpremixed H_2O/CH_4/air flames with R_{H_2O/CH_4} = 0 (a), 0.3 (b) and 0.9 (c) and a = 62 s^{-1}(the volumetric flow rates of CH_4 = 2.4 L/min and oxidizer = 4.4 L/min) at NP, T_F = 550 K and T_O= 350 K. The flames with and without water vapor addition are located on the fuel side of the symmetric plane between the two nozzles. For no water (Fig. 2a) and low (Fig. 2b) water-laden conditions, the flame consists of a blue zone and a yellow luminous zone at the flame wings (edges) and a thin dark zone in between the two zones. With water addition, however, the blue zone is extended, while the yellow luminous zone is reduced. The blue zone is observed closer on the air side of the flame, while the luminous zone is observed on the fuel side. In the blue zone the peak flame temperature is observed and thus primary combustion reactions occur. In the yellow zone, preliminary spectroscopic investigations have shown a presence of sodium (from water and/or impurities inside the burner and on the nozzle exit mesh). Further considerations are necessary to determine if this yellow luminous zone just due to soot particles. Computations were also conducted to study the relationship between the added amount of H_2O vapor and the predicted concentration of C_2H_2 as a gas phase soot marker. These results are not included because of paper length limitations, but the results are consistent with the luminosity coming from incandescent soot, but the results are consistent with the luminosity coming from incandescent soot.

3.2 Extinction limits

Figure 3 shows that T_{max} decreases linearly with increasing R_{H_2O/CH_4} for nonpremixed H_2O/CH_4/air flames of a = 62−108 s^{-1} (=2.4−4.0 L/min and = 4.4−7.5 L/min). The figure shows that for higher strain rates and with no water added the flame temperature is approximately 1850K, whereas for lower strain rates the flame temperatures begin near 1830K. The flames that start at higher strain rates have higher temperatures at extinction due to the smaller amount of thermal heat capacity represented by the water since less water is present at extinction. The lower strain rate flames extinguish at much lower temperatures than the higher strain rate flames. Sung et al. has shown that at higher strain rates the flame thickness decreases causing an increase of reactant leakage that could eventually extinguish the flame [18]. We also see a slight reduction in flame temperature with increasing strain rate, but this change is too slight to observe in our experiments because the inlet gas temperature varies to approximately the same level. This suggests that the reactant leakage is more significant under the high water lade conditions near extinction that at the initial water-free fuel flow condition. In any case, the heated counterflow flames can carry very high levels of water (up to and beyond molar ratios of 2.0) and the flames extinguish at approximately the same temperature (1650−1700 K). The amount of water that can be carried by the fuel without extinguishing the flame increases with decreasing strain rate.

Figure 4 shows the computed T_{max} as a function of R_{H_2O/CH_4} for nonpremixed H_2O/CH_4/air flames at the same experimental conditions shown in Figure 3. Computations for nonpremixed H_2O/CH_4/air flames for a = 50, 100 and 200 s^{-1} were also performed (not shown in this paper) and the trends are consistent. A linear decrease in flame temperature is shown with water addition, except near extinction. The amount of water that can be carried by the fuel without extinguishing the flame increases with decreasing strain rate. The flames extinguish at approximately 100 K lower than is found in the experiment (1550−1590 K). The experimentally observed anomaly that the flame temperature is not necessarily lower with higher strain rate is not observed computationally, where a steady decrease in flame temperature with increasing strain rate at the same level of water addition is seen. The computation does not include the small variations in inlet flow temperature. The major discrepancy between experiment and computation is that T_{max} is overestimated and the experimental flames carry substantially less water at extinction than is predicted. Thus, the flames extinguish at the temperature that is about 100 K higher than is computationally predicted, though T_{max} is overestimated in general.

3.3 Flame structure

Effects of water vapor addition on the structure of nonpremixed CH_4/air flames at NP are given in Fig. 5 and Fig. 6, which show the distribution of temperature and species mole fractions for pure CH_4/air ($R_{H2}O/CH_4$ = 0) and H_2O-added $CH4/air(R_{H2}O/CH_4$= 1.5) flames at two strain rates and at NP, with T_F= 550 K and T_O= 350 K. The computational results indicate that the flames are located on the air (oxygen) side of the stagnation plane. This is a result of the stoichiometry for the reaction between the CH_4 (and H_2O vapor) and air [12]. It should be noted that the stagnation plane is not halfway between the nozzles when the velocities match the stagnation plane is toward the fuel side since the H_2O-CH_4 mixture is less dense than the air. With H_2O addition, T_{max} drops around 200 K and the flame thickness somewhat decreases. The decreased temperature causes radical concentrations, particularly the light radical H, in the reaction zone of the H_2O-added flame to decrease compared with the pure CH_4 flame, decreasing the reactivity for the H_2O-added flame. In low-stretched flames, as in Fig. 6, the T_{max} drops around 230 K and the flame thickness somewhat decreases with H_2O addition. Decreased temperature causes H concentration to decrease. Both the flames with and without H_2O addition are still located on the air side of the stagnation plane due to the stoichiometry for the reaction between the H_2O-CH_4 mixture and air. With increasing strain rate, however, the flame position moves closer to the stagnation plane and the flame thickness decreases due to the enhanced exit velocities at the nozzles, compared with the low-stretch flames in Fig. 6.

Figures 5 and 6 can also help explain the observed soot tendencies with increasing or decreasing R_{H_2O/CH_4}. They show that with water addition more OH radicals are found on the fuel side but with increasing R_{H_2O/CH_4} the peak concentration of OH in the flame decreases.These observations are consistent with the disappearance of the yellow luminous zone in the nonpremixed H_2O/CH_4/air flames as the OH radicals help oxidize soot precursors. Also, flame temperature decreases with increasing R_{H_2O/CH_4}, but effects of the enhanced OH concentration seem to dominate. This finding will be further explored in future work.

In order to separate the thermal and chemical effects of water vapor addition on the structure of a nonpremixed CH_4/air flame an imaginary inert gas X, which has the same thermodynamic and transport properties as those of H_2O, but does not participate in the reaction, was introduced. Due to the reduction of supplied CH_4 with H_2O addition, the flame temperature decreases for both H_2O/CH_4/air and X/CH_4/air flames, compared with pure CH_4/air flames. However, both the H_2O/CH_4/air and X/CH_4/air flames show almost the same structure except for some minor species and water. A similar tendency was observed for most R_{H_2O/CH_4}, which implies that the chemical effects of H_2O addition are far less significant than thermal effects.It should be noted, however, that relatively small changes in species concentrations at the sensitive conditions near extinction can be very important, so further study is needed to quantify the relative significance of direct thermal and chemical effects.

4 Conclusions

The extinction behavior and structure of counterflow nonpremixed water-vapor-laden methane/air flames were experimentally and computationally studied to better understand combustion processes when a large amount of water is naturally incorporated into the fuel stream. For a fixed strain rate, the maximum flame temperature decreases with water addition due to cooling and dilution effects, but under low strain conditions, flames can sustain water beyond molar ratios of 2. The flame becomes thinner with increasing strain rate, which may then lead to an increased amount of reactant leackage and reduction in flame temperature, that then extinguishes the flame entirely. Predictions assuming added water vapor inert indicate that the chemical effects of water addition on flame structure are small and thus the thermal process (i.e., cooling and diluting effects) is mainly involved when water is added to methane/air flames. Also, it is observed that the flame shifts towards the air side nozzle with water addition, indicating that for a fixed methane flow the effects of increased momentum of the water-laden jet (rather than the effects of the stoichiometry for the reaction between the water-laden methane and air) on the flame position are dominant, though the effect is not substantial. Finally, the predicted and measured tendencies of extinction limits and temperature for various conditions show encouraging agreement but quantitative discrepancies among the predictions and measurements merit additional consideration.

5 Acknowledgements

This work was supported by National Research Foundation of Korea Grant funded by the Korean Government (Grant No. 2011−0017880) and by the U.S. National Science Foundation under grant number CBET−0932415 and as part of the California State University, Los Angeles, Center for Energy and Sustainability. The authors appreciate the assistance of Daniel Jaimes in carrying out some of the experiments.

6 Nomenclature

Temperature

T_o	Exit temperature from the oxidizer burner [K]
T_f	Exit temperature from the fuel burner [K]
T_{max}	Maximum temperature at extinction [K]

Gases

N_2	Nitrogen
CH_4	Methane
H_{2O}	Water
C_2H_2	Acetylene

Burner dimensions

d	burner diameter [mm]
L	gap length between oxidizer and fuel burner [mm]

Greek letters

ρ_f	density of fuel [g/cm^3]
ρ_o	density of oxidizer [g/cm^3]

Velocity

u_o	velocity of oxidizer [cm/s]
u_f	velocity of fuel [cm/s]

Flame Properties

a	Strain rate [1/s]
R_{CH_4/H_20}	Methane to Water Molar Ratio

Units

mm	millimiter
in	inches
L/min	Liters per minute

References

[1] C.A. Koh, E.D. Sloan, AIChE J. 53 (2007) 1636−1643.

[2] S. Circone, S.H. Kirby, L.A. Stern, J. Phys. Chem. B 109 (2005) 9468−9475.

[3] A.K. Lazzarini, R.H. Krauss, H.K. Chelliah, G.T. Linteris, Proc. Combust. Inst. 28 (2000) 2939−2945.

[4] G.O. Thomas, Combust. Flame 130 (2002) 147−160.

[5] B. Han, A.F. Ibarreta, C.J. Sung, J.S. T'ien, Combust. Flame 149 (2007) 173−190.

[6] S.C. Li, P.A. Libby, F.A. Williams, Proc. Combust. Inst. 24 (1992) 1503−1512.

[7] J. Park, S.I. Keel, J.H. Yun, Energy Fuels 21 (2007) 3216−3224.

[8] S., Göke, S. Schimek, A. Fateev, S. Clausen, P. Kuhn, S. Terhaar, C.O. Paschereit, Investigation of NOx and CO formation in a premixed swirl-stabilized flame at ultra wet conditions, AIAA 2011−5535, 2011. H.K. Chelliah, C.K. Law, T. Ueda, M.D. Smooke, F.A. Williams, Proc. Combust. Inst. 23 (1990) 503−511.

[9] S. Lee, O.C. Kwon, Int. J. Hydrogen Energy 36 (2011) 10117−10128.

[10] C.E. Lee, S.R. Lee, J.W. Han, J. Park, Int. J. Energy Res. 25 (2001) 343−354.

[11] W. Malkmus, J. Opt. Soc. America 57 (1967) 323−329.

[12] A. Soufiani, J. Taine, Int. J. Heat Mass Trans. 40 (1997) 987−991.

[13] A.E. Lutz, R.J. Kee, J.F. Grcar, F.M. Rupley, OPPDIF: a FORTRAN program for computing opposed-flow diffusion flames, Report No. SAND96−8243, Sandia National Laboratories, 1996.

[14] R.J. Kee, F.M. Rupley, J.A. Miller, The CHEMKIN thermodynamic data base, Report No. SAND87-8215B, Sandia National Laboratories, 1992.

[15] R.J. Kee, F.M. Rupley, J.A. Miller, CHEMKIN II: A FORTRAN chemical kinetics package for the analysis of gas phase chemical kinetics, Report No. SAND89−8009B, Sandia National Laboratories ,1993.

[16] R.J. Kee, G. Dixon-Lewis, J. Warnatz, M.E. Coltrin, J.A. Miller, A FORTRAN computer code package for the evaluation of gas-phase, multi-component transport properties, Report No. SAND86-8246, Sandia National Laboratories, 1992.

[17] M. Frenklach, C.T. Bowman, G.P. Smith, W.C. Gardiner, available at <http://www.me.berkeley. edu/gri mech/>, Version 3.0.

[18] C.J.Sung, J.B. Liu, and C.K. Law. Structural Response of Counterflow Diffusion Flames to Strain Rate Variation. Combustion and Flame 102:481-492 (1995).

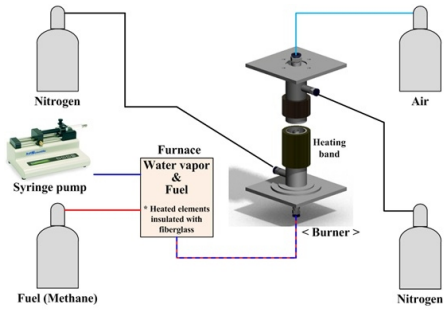

Figure 1: Schematic of experimental apparatus, counterflow burner.

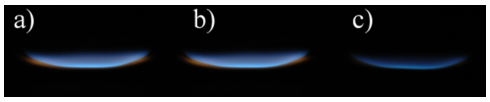

Figure 2: Photographs of counterflow nonpremixed H_2O/CH_4/air flames of $R_{H2O/CH4}$ = 0 (a), 0.3 (b) and 0.9 (c) and a = 62 s^{-1} (= 2.4 L/min and = 4.4 L/min) at NP, T_F = 550 K and T_O= 350 K.

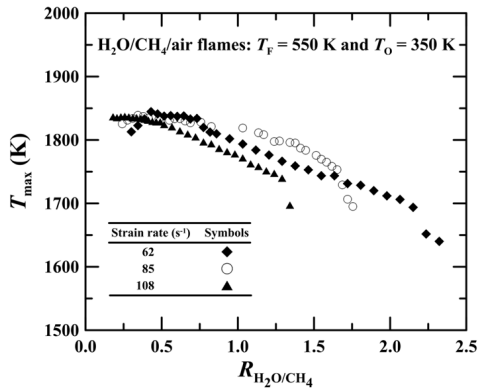

Figure 3: Measured T_{max} as function of $R_{H2O/CH4}$ for nonpremixed H2O/CH4/air flames of a = 62−108 s^{-1} (= 2.4−4.0 L/min and = 4.4−7.5 L/min) at NP, T_F = 550 K and T_O = 350 K.

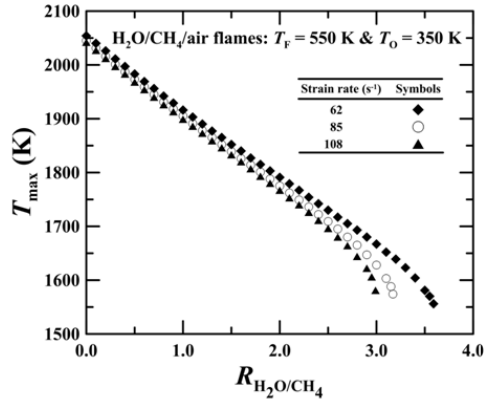

Figure 4: Predicted T_{max} as function of $R_{H2O/CH4}$ for nonpremixed H_2O/CH_4/air flames of a = 62−108 s^{-1} at NP, T_F = 550 K and T_O = 350 K. Based on kinetics of Frenklach et al. [17].

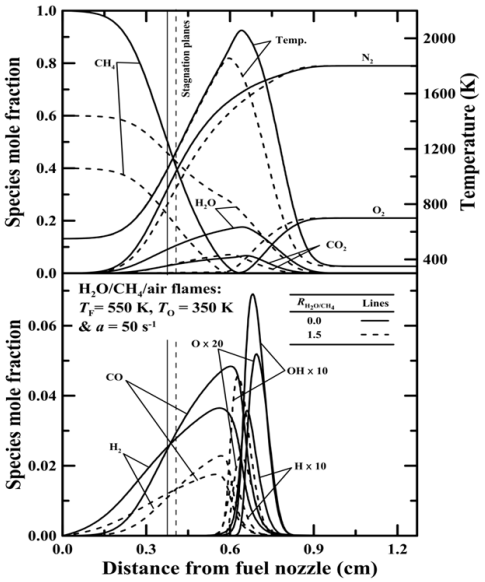

Figure 5: Predicted effects of H_2O addition on structure of low-stretched nonpremixed CH_4/air flame at NP, T_F = 550 K and T_O = 350 K (a = 50 s^{-1}). Based on kinetics of Frenklach et al. [17].

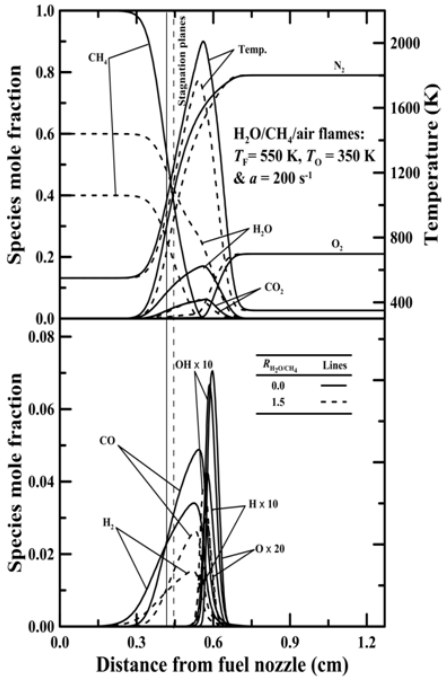

Figure 6: Predicted effects of H_2O addition on structure of high-stretched nonpremixed CH_4/air flame at NP, T_F = 550 K and T_O = 350 K (a = 200 s^{-1}). Based on kinetics of Frenklach et al. [17].